Anomalies in the specific heat of a free damped particle: the role of the cutoff in the spectral density of the coupling

Benjamin Spreng[1], **Gert-Ludwig Ingold**[1] **and Ulrich Weiss**[2]

[1] Institut für Physik, Universität Augsburg, D-86135 Augsburg, Germany
[2] Institut für Theoretische Physik, Universität Stuttgart, D-70550 Stuttgart, Germany

E-mail: gert.ingold@physik.uni-augsburg.de

Abstract

The properties of a dissipative system depend on the spectral density of the coupling to the environment. Mostly, the dependence on the low-frequency behavior is in the focus of interest. However, in order to avoid divergencies, it is also necessary to suppress the spectral density of the coupling at high frequencies. Interestingly, the very existence of this cutoff may lead to a mass renormalization which can have drastic consequences for the thermodynamic properties of the dissipative system. Here, we explore the role which the cutoff in the spectral density of the coupling plays for a free damped particle and we compare the effect of an algebraic cutoff with that of a sharp cutoff.

Keywords: quantum dissipation, thermodynamics anomalies, specific heat

1. Introduction

In the study of dissipative systems the case of strictly Ohmic damping plays a prominent role because it implies memoryless damping. However, this model is the result of an idealization which assumes that the density of the environmental modes weighted by the coupling strength increases proportional to the frequency even for arbitrarily large frequencies. In realistic scenarios, this will not be the case and, on a more formal level, it can give rise to divergencies. Therefore, one is usually obliged to introduce a high-frequency cutoff in the spectral density of the coupling. Often one can assume that the cutoff represents the largest frequency scale in the problem and that the resulting memory time of the damping is shorter than any time scale of interest.

While the cutoff in the spectral density of the coupling usually only leads to quantitative changes of relatively little physical interest, occasionally the presence of a cutoff can make a qualitative difference. Here, we will consider such a situation. The thermodynamic properties of a free damped particle at low temperatures depend significantly on an environment-induced renormalization of the particle's mass. In particular, there exists a regime, where the mass renormalization can be negative and thus reduces the mass of the particle. When the renormalized mass becomes negative, one observes anomalies like a negative specific heat [1]. Such anomalies in the specific heat and in the entropy are of interest in various contexts [2–8].

The mass renormalization alluded to here is due to the suppression of the density of high-frequency environmental modes and thus is a direct consequence of the very existence of a cutoff in the spectral density of the coupling.

We will consider in this paper the specific heat of a free Brownian particle subject to a linear environment where the spectral density of the coupling at low frequencies follows a general power law. At high frequencies we allow either for an algebraic cutoff which in the simplest case will take the form of a Drude cutoff or for a sharp cutoff where no environmental modes are assumed to be present above a certain cutoff frequency. It will become clear that these two cutoff functions can lead to quantitatively quite different results. In particular, we will find that for a sharp cutoff the appearance of a negative specific heat cannot be inferred from the leading low-temperature behavior.

Before embarking on our study, we need to say a few words about the meaning of a negative specific heat which usually should provoke worries about thermodynamic instability. However, here we are referring to the specific heat

of a system degree of freedom coupled to an environment. It turns out that beyond weak coupling, the specific heat of a dissipative quantum system is not uniquely defined [9]. Here, we will base our considerations on the reduced partition function

$$\mathcal{Z} = \frac{\mathcal{Z}_{\mathrm{S+B}}}{\mathcal{Z}_{\mathrm{B}}}, \tag{1}$$

where $\mathcal{Z}_{\mathrm{S+B}}$ is the partition function of the coupled ensemble of system and bath while $\mathcal{Z}_{\mathrm{B}}$ refers to the partition function of the bath alone. In the absence of any coupling between system and bath, the reduced partition function clearly agrees with the partition function of the system alone.

We can now employ standard relations of thermodynamics to obtain any thermodynamic quantity from the reduced partition function (1). The resulting quantities have a clear physical significance as the difference between the quantity of system and bath and the same quantity determined for the bath alone. For the specific heat, we have [10]

$$C = C_{\mathrm{S+B}} - C_{\mathrm{B}}. \tag{2}$$

While each of the terms, $C_{\mathrm{S+B}}$ and C_{B}, has to be positive, their difference can very well become negative and in fact it does under appropriate circumstances. The physical reason is the suppression of the bath density of states at low frequencies when the system degree of freedom is coupled to it [11]. How strongly the bath density of states will be suppressed depends directly on the high-frequency cutoff of the spectral density of the coupling.

We start in section 2 by introducing general concepts needed to describe the damped free particle. In particular, we will introduce the spectral density of the coupling for the two models with, on the one hand, an algebraic cutoff and, on the other hand, a sharp cutoff. The corresponding spectral damping functions will be deduced and their properties will be presented. The section closes with a discussion of the mass renormalization associated with the two models. This quantity will play an important role for the thermodynamic anomalies in the specific heat. Section 3 is devoted to the change of the bath density of states when the free particle is coupled to it. Special attention will be paid to the differences between the two models for the cutoff. In section 4 we introduce the reduced partition function of the damped free particle which will constitute the basis of the calculation of the specific heat. We will demonstrate how the specific heat can be expressed either in terms of the spectral damping function or the change in the bath density of states obtained in section 3. Sections 5 and 6 are devoted to the behavior of the specific heat at high and low temperatures, respectively. We close by presenting our conclusions in section 7.

2. Free Brownian particle subject to general linear damping

2.1. Spectral density of the coupling

We assume that the free Brownian particle is moving in one spatial dimension and is subject to a linear but otherwise general damping mechanism. Its classical or quantum average velocity then obeys the equation of motion

$$\langle \dot{v} \rangle(t) + \int_{-\infty}^{t} \mathrm{d}s\, \gamma(t-s) \langle v \rangle(s) = 0. \tag{3}$$

Here, $\gamma(t)$ is the damping kernel which in the following will mostly appear in the form of its Laplace transform, the spectral damping function $\hat{\gamma}(z)$. All properties of the damped free particle can be expressed in terms of the causal velocity response function $\mathcal{R}(t)$ whose Laplace transform can immediately be read off from (3) as

$$\hat{\mathcal{R}}(z) = \frac{1}{z + \hat{\gamma}(z)}. \tag{4}$$

The two terms in the denominator are associated with the inertia term and the damping term, respectively.

Although in principle it is sufficient to specify the spectral damping function $\hat{\gamma}(z)$, it is useful to consider an explicit model leading to (3). Doing so will allow to more systematically define the damping mechanism and to give a more physical interpretation of the results. A free damped particle of mass M subject to linear damping can always be modelled by a Hamiltonian in which the particle described by its position Q and momentum P is coupled bilinearly to a set of harmonic oscillators with masses m_n and frequencies ω_n described by their positions q_n and momenta p_n [12]

$$H = \frac{P^2}{2M} + \sum_{n=1}^{\infty} \left[\frac{p_n^2}{2m_n} + \frac{m_n \omega_n^2}{2} \left(q_n - Q \right)^2 \right]. \tag{5}$$

In general, the coupling of a system to an environment will lead to a potential renormalization for which we have accounted here by choosing a translationally invariant Hamiltonian. Although the masses m_n and frequencies ω_n give large freedom to choose a Hamiltonian, it turns out that the only quantity of relevance for the properties of the free damped particle is the spectral density of the coupling [13, 14]

$$J(\omega) = \frac{\pi}{2} \sum_{n=1}^{\infty} m_n \omega_n^3 \delta(\omega - \omega_n). \tag{6}$$

In particular, the spectral damping function can be obtained from it according to

$$\hat{\gamma}(z) = \frac{2}{\pi M} \int_0^{\infty} \mathrm{d}\omega\, \frac{J(\omega)}{\omega} \frac{z}{\omega^2 + z^2}. \tag{7}$$

A property of the bath which will be of relevance later on is its total mass

$$M_{\mathrm{bath}} \equiv \sum_{n=1}^{\infty} m_n = \frac{2}{\pi} \int_0^{\infty} \mathrm{d}\omega\, \frac{J(\omega)}{\omega^3}. \tag{8}$$

In the following, we will specify the damping mechanism through its spectral density. We assume the spectral distribution of bath oscillators to be continuous and to follow a power law at low frequencies

$$J_0(\omega) = M\gamma\omega \left(\frac{\omega}{\omega_{\mathrm{c}}} \right)^{s-1}. \tag{9}$$

The exponent s thus specifies the low-frequency behavior. The regimes $s < 1$ and $s > 1$ correspond to sub-Ohmic and super-Ohmic damping, respectively, and $s = 1$ is the special case of Ohmic damping.

To obviate divergences of spectral integrals for observables, the actual spectral density must fall off sufficiently strong in the limit $\omega \to \infty$. This may be taken into account by equipping $J_0(\omega)$ with a cutoff function $f(\omega/\omega_c)$ which approaches unity in the limit $\omega/\omega_c \to 0$, and drops to zero sufficiently fast as ω/ω_c goes to infinity. Hence we put

$$J(\omega) = J_0(\omega) f(\omega/\omega_c). \tag{10}$$

Without restriction of generality, the reference frequency ω_c in $J_0(\omega)$ is identified with the cutoff frequency in $f(\omega/\omega_c)$. In the sequel, we consider both a smooth and a sharp cutoff of the spectral bath coupling at high frequencies. For the sake of simplicity, we use from now on units where $\omega_c = k_B = \hbar = 1$.

2.2. Spectral density with algebraic cutoff (model I)

To be specific, we choose for the case of a smooth cutoff the algebraic function $f(x) = 1/(1 + x^2)^p$, yielding

$$J_{ac}(\omega) = \frac{J_0(\omega)}{\left[1 + (\omega/\omega_c)^2\right]^p}. \tag{11}$$

We will use the subscript 'ac' to indicate that a quantity is taken for the algebraic cutoff. Occasionally, we omit the subscript when the context permits it.

The frequency integral (7) with (11) is convergent for s in the range

$$0 < s < 2p + 2 \tag{12}$$

and can be expressed in terms of hypergeometric functions. The resulting expression with a convergent hypergeometric series in the regime $|z| > 1$ is

$$\hat{\gamma}(z) = \frac{\gamma}{\sin\left(\frac{\pi s}{2}\right)} \frac{z^{s-1}}{\left(1 - z^2\right)^p} + \frac{\gamma}{\pi z} B\left(p - \tfrac{s}{2}, \tfrac{s}{2}\right) {}_2F_1\left(1, \tfrac{s}{2}; 1 - p + \tfrac{s}{2}; z^{-2}\right). \tag{13}$$

Here, ${}_2F_1$ denotes the hypergeometric function and the function $B(x, y)$ is Euler's beta function [15].

By use of a linear transformation, the second term in equation (13) can be rewritten as a hypergeometric series which is convergent in the regime $|z| < 1$,

$$\hat{\gamma}(z) = \frac{\gamma}{\left(1 - z^2\right)^p} \left[\frac{z^{s-1}}{\sin\left(\frac{\pi s}{2}\right)} + \frac{2p}{\pi} \frac{B\left(p + 1 - \frac{s}{2}, \frac{s}{2}\right)}{s - 2} \times z\, {}_2F_1\left(1 - p, 1 - \tfrac{s}{2}; 2 - \tfrac{s}{2}; z^2\right) \right]. \tag{14}$$

For integer p, the ${}_2F_1$ function in (14) is a terminating hypergeometric series

$$\hat{\gamma}(z) = \frac{\gamma}{\left(1 - z^2\right)^p} \left[\frac{z^{s-1}}{\sin\left(\frac{\pi s}{2}\right)} + \frac{1}{\pi} \sum_{n=0}^{p-1} \frac{(-1)^{n-1}}{n + 1 - \frac{s}{2}} \frac{B\left(\frac{s}{2}, p + 1 - \frac{s}{2}\right)}{B(n + 1, p - n)} z^{2n+1} \right]. \tag{15}$$

The forms (13) and (14) or (15) allow us to easily read off the behaviors of $\hat{\gamma}(z)$ for large and small arguments. These will be needed in sections 5 and 6 to determine the specific heat at high and low temperatures, respectively.

Under the tighter constraint

$$0 < s < 2p, \tag{16}$$

the integral $\int_0^\infty d\omega\, J(\omega)/\omega$ is consistently ultraviolet-convergent. As a result, the leading contribution to $\hat{\gamma}(z)$ at high frequencies, $z \gg 1$, is proportional to $1/z$,

$$\hat{\gamma}(z) = \frac{2}{\pi M} \int_0^\infty d\omega \frac{J(\omega)}{\omega} \frac{1}{z} = \frac{a}{z}, \tag{17}$$

where for model I

$$a_{ac}(s, p) = \gamma \frac{B\left(p - \frac{s}{2}, \frac{s}{2}\right)}{\pi}. \tag{18}$$

The $1/z$-term of $\hat{\gamma}(z)$ determines the high-temperature behavior of the damped particle, as we shall see in section 5.

On the other hand, the low-temperature properties of the free damped particle are determined by the low-frequency characteristics of $\hat{\gamma}(z)$. We obtain for $|z| \ll 1$

$$\hat{\gamma}_{ac}(z) = \frac{\gamma z^{s-1}}{\sin\left(\frac{\pi s}{2}\right)} \left(1 + p z^2\right) + \mu_{ac} z + \lambda_{ac} z^3, \tag{19}$$

where the orders z^{s+3}, z^5, and higher are disregarded. We have

$$\mu_{ac}(s, p) = \frac{2\gamma}{\pi} \frac{p\, B\left(\frac{s}{2}, 1 + p - \frac{s}{2}\right)}{s - 2}, \tag{20}$$

and

$$\lambda_{ac}(s, p) = -\mu_{ac}(s - 2, p) = \frac{2\gamma}{\pi} \frac{p B\left(\frac{s}{2} - 1, 2 + p - \frac{s}{2}\right)}{4 - s}. \tag{21}$$

The first term in (19), in which we have included the leading cutoff dependence, describes frequency-dependent damping. The second term adds to the inertial term z in the denominator of $\hat{\mathcal{R}}(z)$. Its prefactor $\mu = \Delta M/M$ can therefore be interpreted as an effective change ΔM of the particle's mass relative to the bare mass M due to the coupling to the environment. This mass renormalization term will be

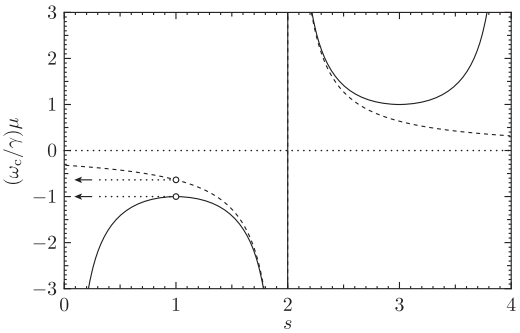

Figure 1. Mass renormalization μ as a function of the exponent s of the spectral density of the coupling $J(\omega)$. The solid curve depicts μ/γ for an algebraic cutoff with $p = 1$ according to (20) while the dashed curve refers to the sharp cutoff, i.e. the expression (30). The two small circles indicate how the critical value of the damping strength $\gamma^\star$ can be read off for $s = 1$. For the algebraic cutoff with $p = 1$ one finds $\gamma^\star_{\rm ac}(1, 1) = \omega_c$, while for the sharp cutoff $\gamma^\star_{\rm sc}(1) = (\pi/2)\omega_c$.

discussed in more detail in section 2.4. Finally, the last term becomes relevant for low temperatures in the regime $0 < s < 2$ at the particular damping strength for which $\mu = -1$, as we shall see.

In the limit $s \to 2m$, where m is a positive integer, both the first term and the term of order z^{2m-1} in the square bracket of (15) become singular. The singularities cancel each other, however, and a logarithmic term accrues. For the particular cases $s = 2$ and $s = 4$ we have

$$\hat\gamma(z) = \frac{\gamma}{\pi}\frac{z}{\left(1-z^2\right)^p}\Big[\psi(1) - \psi(p) - 2\ln(z) + (p-1)z^2\,{}_3F_2\Big(1, 1, 2-p; 2, 2; z^2\Big)\Big] \tag{22}$$

and

$$\hat\gamma(z) = \frac{\gamma}{\pi}\frac{z}{\left(1-z^2\right)^p}\left\{\frac{1}{p-1} + z^2[2\ln(z) + \psi(p-1) - \psi(1) - 1] + \left(1-\tfrac{p}{2}\right)z^4\,{}_3F_2\Big(1, 1, 3-p; 2, 3; z^2\Big)\right\}, \tag{23}$$

respectively, where $\psi(z)$ is the digamma function [15].

2.3. Spectral density with sharp cutoff (model II)

Concerning our study to which extent thermodynamic properties depend on the particular form chosen for the cutoff in the spectral coupling, we contrast the smooth cutoff function discussed in the previous section with a sharp cutoff function $f(x) = \Theta(1-x)$, where $\Theta(x)$ denotes the Heaviside step function. Together with the spectral coupling (9) we have

$$J_{\rm sc}(\omega) = J_0(\omega)\Theta\big(1 - \omega/\omega_c\big), \tag{24}$$

where the subscript 'sc' indicates the sharp cutoff. From now on we set again $\omega_c = 1$. The sharp cutoff in the spectral density (24) is in striking contrast to the smooth cutoff in equation (11).

For the spectral density (24), the frequency integral in the expression (7) for the spectral damping function $\hat\gamma(z)$ can again be expressed in terms of hypergeometric functions. In the frequency regime $|z| > 1$ one finds

$$\hat\gamma(z) = \frac{2\gamma}{\pi}\frac{{}_2F_1\Big(1, \frac{s}{2}; 1+\frac{s}{2}; -z^{-2}\Big)}{sz}. \tag{25}$$

Convergence of the hypergeometric series in the complementary regime $|z| < 1$ is obtained by virtue of a linear transformation of the ${}_2F_1$ function in equation (25), yielding

$$\hat\gamma(z) = \frac{\gamma z^{s-1}}{\sin\left(\frac{\pi s}{2}\right)} + \frac{2\gamma}{\pi}z\frac{{}_2F_1\Big(1, 1-\frac{s}{2}; 2-\frac{s}{2}; -z^2\Big)}{s-2}. \tag{26}$$

In the particular cases $s = 1$ and $s = 3$, the spectral damping function reads

$$\hat\gamma(z, s=1) = \gamma - \frac{2\gamma}{\pi}\arctan(z),$$
$$\hat\gamma(z, s=3) = \frac{2\gamma}{\pi}\left[z - z^2\left(\frac{\pi}{2} - \arctan(z)\right)\right], \tag{27}$$

respectively.

The asymptotic high-frequency expression of $\hat\gamma(z)$ may be written in the form (17) with the coefficient

$$a_{\rm sc}(s) = \frac{2\gamma}{\pi s}. \tag{28}$$

Similar to equation (19), the low-frequency expansion may be expressed as

$$\hat\gamma_{\rm sc}(z) = \frac{\gamma z^{s-1}}{\sin\left(\frac{\pi s}{2}\right)} + \mu_{\rm sc}z + \lambda_{\rm sc}z^3, \tag{29}$$

where terms of order z^5 are disregarded. For model II, the relative mass contribution μ and the prefactor of the z^3-term are

$$\mu_{\rm sc}(s) = \frac{2\gamma}{\pi(s-2)}, \tag{30}$$

and

$$\lambda_{\rm sc}(s) = -\mu_{\rm sc}(s-2) = \frac{2\gamma}{\pi(4-s)}. \tag{31}$$

2.4. Mass renormalization

The linear term in z in equations (19) and (29) contributes to the inertial term in the Laplace transform (4) of the velocity response function. It thus leads to a mass renormalization which will turn out to be of relevance for the thermodynamic properties of the free damped particle. We distinguish the regimes $s < 2$ and $s > 2$ and start our discussion with the latter. Before, we remark though that the motion of a free damped particle in the regime $s > 2$ is non-ergodic so that thermodynamic equilibrium is not necessarily being reached in the long-time limit [16, 17].

In the parameter regime $s > 2$ the linear term in z of $\hat\gamma(z)$ is the leading one in (19) and (29) for $z \ll 1$. Together with

(7) and (8) one generally finds

$$\hat{\gamma}'(0) = \mu = \frac{M_{\rm bath}}{M}, \tag{32}$$

where the prime denotes the derivative with respect to the argument. The results (20) and (30) are special cases of the general expression (32). For $s > 2$, the dressed mass $M(1+\mu)$ is larger than the particle's bare mass M, since μ is always positive. The free particle can thus be viewed as dressed by the bath oscillators. For $s > 2$, the appearance of an effective mass is also known for the ballistic long-time dynamics of the free damped particle [18].

The relative mass renormalization μ is depicted in figure 1 as a function of the exponent s both for an algebraic cutoff with $p = 1$ (solid line) and a sharp cutoff (dashed line). For $s > 2$, i.e. in the right half of the diagram, we notice a significant difference between the algebraic and the sharp cutoff. In the first case, with increasing exponent s, the mass renormalization goes through a minimum and diverges at the upper limit of the allowed range (12) at $2p + 2$. For the case $p = 1$ presented in the figure, the divergence lies at $s = 4$. In contrast, the mass renormalization for the sharp cutoff decreases monotonically as s increases. We remark that although for $p = 1$ the mass renormalization for an algebraic cutoff always exceeds the one for the sharp cutoff, this is generally not true for larger values of p.

For $s \leqslant 2$, the integral (8) is infrared-divergent so that the total mass of the bath oscillators is infinite. Hence the interpretation just given for the relative mass contribution μ ceases to hold. Nevertheless, the expressions (20), (30), and (32) can be analytically continued to the regime $0 < s < 2$. To show this, we write $J(\omega) = J_0(\omega) - [J_0(\omega) - J(\omega)]$. For $s < 2$, substitution of the expression (9) for $J_0(\omega)$ in (7) results in the first term appearing in the series expressions (19) and (29). With the residual contribution of $J(\omega)$, the integral expression (7) is regular in linear order of z and yields μz in this order. Importantly, the mass contribution μ emerges negative

$$\begin{aligned}\mu &= \frac{2}{\pi M}\int_0^\infty {\rm d}\omega \frac{J(\omega) - J_0(\omega)}{\omega^3} \\ &= \frac{M_{\rm bath} - M_{\rm bath,0}}{M} < 0.\end{aligned} \tag{33}$$

The relation (33) unveils that $-\mu M$ represents the total mass of oscillators which is missing in the actual bath relative to the reference bath without spectral cutoff [11, 19]. Hence μ is negative in the range $0 < s < 2$, as can also be seen from the left half of figure 1. Again, we note significant differences between the algebraic cutoff and the sharp cutoff. While the first one goes through a minimum in the absolute value of μ, for the latter the mass renormalization becomes the smallest for $s \to 0$.

As can be expected, the situation where the particle's mass is renormalized to zero, i.e. where $\mu = -1$, is of special physical significance. It is therefore convenient, to introduce the critical damping strength $\gamma^\star$, where this point is reached,

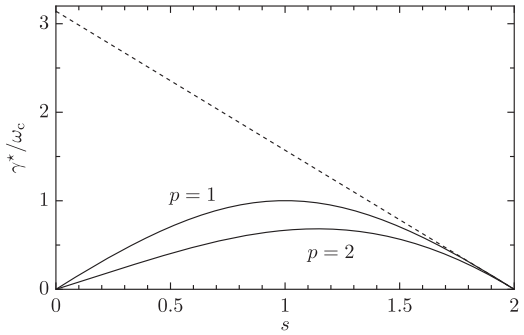

Figure 2. Critical damping strength $\gamma^\star$ as a function of the exponent s in the regime $0 < s < 2$. The two solid curves show $\gamma^\star_{\rm ac}$ (model I) for $p = 1$ (upper curve) and p=2 (lower curve) while the dashed line depicts $\gamma^\star_{\rm sc}$ (model II).

as

$$1 + \mu = 1 - \frac{\gamma}{\gamma^\star}, \tag{34}$$

and thus

$$\gamma^\star = -\frac{\gamma}{\mu}. \tag{35}$$

The two circles and the arrows pointing to the vertical axis in figure 1 indicate, how the inverse of the critical value $\gamma^\star$ can be read off for $s = 1$. The comparison of the algebraic cutoff with $p = 1$ (solid curve) and the sharp cutoff (dashed curve) indicates that for the latter, a larger damping strength is required to drive the renormalized mass to zero. Explicit expressions for the critical damping strength can be obtained for our two models from the expressions (20) and (30) for the relative mass contribution. For an algebraic cutoff (model I), one obtains

$$\gamma^\star_{\rm ac}(s, p) = \pi\left(1 - \tfrac{s}{2}\right)\frac{\Gamma(p)}{\Gamma\left(1 + p - \frac{s}{2}\right)\Gamma\left(\frac{s}{2}\right)}. \tag{36}$$

while for the sharp cutoff (model II) the critical damping strength follows as

$$\gamma^\star_{\rm sc}(s) = \pi\left(1 - \tfrac{s}{2}\right). \tag{37}$$

The critical damping strength $\gamma^\star$ is plotted in figure 2 both for model I with cutoff parameters $p = 1$ and $p = 2$ (solid curves) and for model II (dashed curve). We see that indeed the critical damping strength for model II is generally larger than for model I. For Ohmic damping, the critical damping strength is typically of the order of the cutoff frequency and it is therefore not surprising, that the cutoff influences the thermodynamic quantities in a significant way. However, when the exponent s approaches a value of 2 or, in the case of an algebraic cutoff, approaches zero, the critical damping strength can be much smaller than the cutoff frequency.

We finally allude again that the notion of a critical damping strength $\gamma^\star$ becomes meaningless in the regime $s \geqslant 2$, since there the analytical continuation, inter alia of (36) or (37), yields a negative value for $\gamma^\star$.

3. Change of bath density of states

3.1. General considerations

There are two different views about the specific heat of an open quantum system: (i) it can be viewed as specific heat of the system modified by the coupling to the heat bath. (ii) It can be regarded as the change in the specific heat of the bath when the system degree of freedom is coupled to it as represented in equation (2). In the latter view which will be discussed in more detail in section 4, the specific heat of the damped free particle can be expressed in terms of the change of the density of states of the bath oscillators together with the well-known expression for the specific heat of a harmonic oscillator. The change in the oscillator density of states (CODS) is defined as

$$\xi(\omega) = \sum_{n'=0}^{\infty} \delta(\omega - \bar{\omega}_{n'}) - \sum_{n=1}^{\infty} \delta(\omega - \omega_n), \tag{38}$$

where $\bar{\omega}_{n'}$ are the eigenvalues of the coupled system-plus-bath complex (5), while ω_n are the eigenfrequencies of the bath oscillators in the absence of the system–bath coupling, i.e. the frequencies appearing in the second term of the Hamiltonian (5). In the absence of the system–reservoir coupling, the CODS reduces for the model (5) to $\xi(\omega) = \delta(\omega)$. In the continuum limit of the bath, the density $\xi(\omega)$ becomes a continuous function of the frequency ω.

The change of the oscillator density of states can be expressed in terms of the velocity response function (4) as

$$\xi(\omega) = \frac{1}{\pi} \operatorname{Im} \frac{\partial \ln\left[\hat{\mathcal{R}}(-\mathrm{i}\omega)\right]}{\partial \omega}, \tag{39}$$

where Im denotes the imaginary part. In terms of the function

$$g(\omega) = \frac{\omega - \operatorname{Im} \tilde{\gamma}(\omega)}{\operatorname{Re} \tilde{\gamma}(\omega)}, \tag{40}$$

where $\tilde{\gamma}(\omega) = \hat{\gamma}(-\mathrm{i}\omega)$ is the spectral damping function in Fourier space, the CODS $\xi(\omega)$ takes the form

$$\xi(\omega) = \frac{1}{\pi} \frac{g'(\omega)}{1 + g(\omega)^2} = \frac{1}{\pi} \frac{\mathrm{d}}{\mathrm{d}\omega} \arctan[g(\omega)]. \tag{41}$$

With the second form, we directly see that the sum rule for the change of the oscillator density of states reads

$$\begin{aligned} \Sigma &\equiv \int_0^{\infty} \mathrm{d}\omega\, \xi(\omega) \\ &= \frac{1}{\pi}(\arctan[g(\infty)] - \arctan[g(0)]). \end{aligned} \tag{42}$$

In section 4 we will see that this sum rule relates the specific heat in the classical limit with its zero-temperature value.

We will now give expressions for the low-frequency behavior of the change of the oscillator density of states which pertain to both cutoffs discussed in the present paper. In the subsequent two subsections, we will take a more detailed look at each of the two models.

The leading terms of the low frequency series of $g(\omega)$ are found from its definition (40) together with equation (19) for model I and equation (29) for model II as

$$\begin{aligned} g(\omega) = &-\cot\left(\frac{\pi s}{2}\right) \\ &+ \frac{1+\mu}{\gamma}\omega^{2-s} - \frac{\Lambda}{\gamma}\omega^{4-s}. \end{aligned} \tag{43}$$

For the models I and II we have, respectively

$$\begin{aligned} \Lambda_{\mathrm{ac}} &= \lambda_{\mathrm{ac}} - p\left(1 + \mu_{\mathrm{ac}}\right), \\ \Lambda_{\mathrm{sc}} &= \lambda_{\mathrm{sc}}. \end{aligned} \tag{44}$$

In the regime $0 < s < 2$, the leading terms of the low-frequency series of $\xi(\omega)$ up to and including ω^{3-s} are found from (41) with (43) as

$$\xi(\omega) = \omega^{1-s}\left[\frac{2-s}{\pi}\sum_{n=0}^{N_1} b_n \left(\frac{1}{\gamma} - \frac{1}{\gamma^{\star}}\right)^{n+1} \omega^{(2-s)n} + c\,\omega^2\right]. \tag{45}$$

Here, the upper limit of summation N_1 is given by the largest integer smaller than $1 + 1/(2-s)$. Thus, the closer to 2 the parameter s is, the more terms of the sum must be taken into account.

The first three coefficients of the first term are

$$\begin{aligned} b_0 &= \sin^2\left(\tfrac{\pi s}{2}\right), \\ b_1 &= \sin^2\left(\tfrac{\pi s}{2}\right)\sin\left(\pi s\right), \\ b_2 &= [1 + 2\cos(\pi s)]\sin^4\left(\tfrac{\pi s}{2}\right), \end{aligned} \tag{46}$$

and the coefficient c is

$$c = -\frac{(4-s)\sin^2\left(\frac{\pi s}{2}\right)}{\pi}\frac{\Lambda}{\gamma}. \tag{47}$$

For the models I and II, Λ is given by (44).

The leading term proportional to ω^{1-s} of the series (45) is positive for $\gamma < \gamma^{\star}$ and negative for $\gamma > \gamma^{\star}$. At critical damping, $\gamma = \gamma^{\star}$, the first term in the square brackets in (45) vanishes, so that the leading term for critical damping is given by

$$\xi(\omega) = c^{\star}\omega^{3-s} \tag{48}$$

with

$$c^{\star} = -\frac{(4-s)\sin^2\left(\frac{\pi s}{2}\right)}{\pi}\frac{\lambda}{\gamma}. \tag{49}$$

The ratio λ/γ in $c^{\star}$ does not depend on the damping strength for both models, as we can see from (21) and (31).

In the Ohmic case, the $n = 2$ term merges with the last term in the series (45) for $\xi(\omega)$ to the curvature contribution at $\omega = 0$. With (46) and (47), we find

$$\xi(\omega) = \frac{1}{\pi}\left(\frac{1}{\gamma} - \frac{1}{\gamma^{\star}}\right) - \frac{1}{\pi}\left[\frac{3\Lambda}{\gamma} + \left(\frac{1}{\gamma} - \frac{1}{\gamma^{\star}}\right)^3\right]\omega^2. \tag{50}$$

Consider finally the regime $s > 2$. Now, the low-frequency expression analogous to (45) with terms of order up to

and including ω^{s-1} reads

$$\xi(\omega) = \omega^{s-3}\Bigg[-\frac{s-2}{\pi}\sum_{n=0}^{N_2} d_n \times \left(\frac{\gamma}{1+\mu}\right)^{n+1} \omega^{(s-2)n} + f\omega^2\Bigg]. \tag{51}$$

The upper limit of summation is given by the largest integer smaller than $2/(s-2)$ and the coefficients read

$$\begin{aligned} d_0 &= 1 \\ d_1 &= 2\cot\left(\tfrac{\pi s}{2}\right) \\ d_2 &= 3\cot^2\left(\tfrac{\pi s}{2}\right) - 1, \end{aligned} \tag{52}$$

and

$$f = -\frac{s}{\pi}\frac{\gamma\Lambda}{(1+\mu)^2}. \tag{53}$$

For super-Ohmic damping with $s = 3$, the $n = 2$ term in (51) again merges with the last term to the curvature contribution at $\omega = 0$. With the expressions (52) and (53) we then find

$$\xi(\omega) = -\frac{\gamma}{\pi(1+\mu)} + \frac{\gamma}{\pi}\frac{\gamma^2 - 3\Lambda(1+\mu)}{(1+\mu)^3}\omega^2. \tag{54}$$

3.2. Model I

We now turn to a more specific discussion of the change of the oscillator density of states for the case of an algebraic cutoff. With the expression (14) for $\hat{\gamma}(z)$, the function $g(\omega)$ for model I is found to read

$$\begin{aligned} g(\omega) = &-\cot\left(\frac{\pi s}{2}\right) + \frac{1}{\gamma}\omega^{2-s}\left(1+\omega^2\right)^p \\ &- \frac{2p}{\pi(2-s)}B\left(p+1-\frac{s}{2}, \frac{s}{2}\right) \\ &\times\ \omega^{2-s}\,{}_2F_1\left(1-p, 1-\tfrac{s}{2}; 2-\tfrac{s}{2}; -\omega^2\right). \end{aligned} \tag{55}$$

The function $g(\omega)$ is a smooth function of ω in the range $0 \leqslant \omega < \infty$. It goes to infinity both in the limit $\omega \to \infty$ for all $s > 0$, and in the limit $\omega \to 0$ for $s \geqslant 2$, whereas $g(\omega = 0) = \cot(\pi\frac{s}{2})$ for $s < 2$. Hence the sum rule (42) reads

$$\Sigma(s) = \left(1 - \frac{s}{2}\right)\Theta(2-s). \tag{56}$$

The low-frequency expansion of the CODS $\xi(\omega)$ in the regime $0 < s < 2$ follows from the expressions (45), (46), and (47) together with (44), (20) and (21). In the first term in (45), the form of the cutoff enters only through the critical damping strength $\gamma_{\rm ac}^\star$. The leading term $n = 0$ in the sum is positive for $\gamma < \gamma_{\rm ac}^\star$ and changes its sign at the critical damping strength $\gamma_{\rm ac}^\star$. The coupling of the system degree of freedom to the heat bath thus leads to a suppression of the oscillator density if the damping exceeds $\gamma_{\rm ac}^\star$. The coefficient c in the second term in (45) takes the form

$$c_{\rm ac} = \frac{\sin^2\left(\frac{\pi s}{2}\right)}{\pi}\left[p(4-s)\left(\frac{1}{\gamma} - \frac{1}{\gamma_{\rm ac}^\star}\right) + \frac{2+2p-s}{\gamma_{\rm ac}^\star}\right]. \tag{57}$$

It is positive for $\gamma < \bar{\gamma}$ and negative for $\gamma > \bar{\gamma}$, where $\bar{\gamma} = \gamma_{\rm ac}^\star p(4-s)/[(p-1)(2-s)]$.

For critical damping, $\gamma = \gamma_{\rm ac}^\star$, the coefficient $c^\star$ in the expression (48) follows from (57) as

$$c_{\rm ac}^\star(s, p) = \frac{\sin^2\left(\frac{\pi s}{2}\right)}{\pi}\frac{2+2p-s}{\gamma_{\rm ac}^\star(s, p)}. \tag{58}$$

This coefficient is always positive since the parameters s and p have to satisfy the condition (12). In particular, for Ohmic damping with a Drude cutoff, $s = 1$ and $p = 1$, we have

$$c_{\rm ac}^\star(1, 1) = \frac{3}{\pi}. \tag{59}$$

The CODS $\xi(\omega)$ is shown for $s = 1$ and $p = 1$ in figure 3(a). In this particular case, in which $\gamma_{\rm ac}^\star = 1$, the low frequency expression (50) takes the form

$$\xi(\omega) = \frac{1}{\pi}\left[\frac{1-\gamma}{\gamma} + \frac{\gamma^3 + 3\gamma - 1}{\gamma^3}\omega^2\right]. \tag{60}$$

This expression describes the low-frequency behavior of the curves in figure 3(a). While $\xi(0)$ changes its sign at the critical damping strength, the curvature at $\omega = 0$ changes

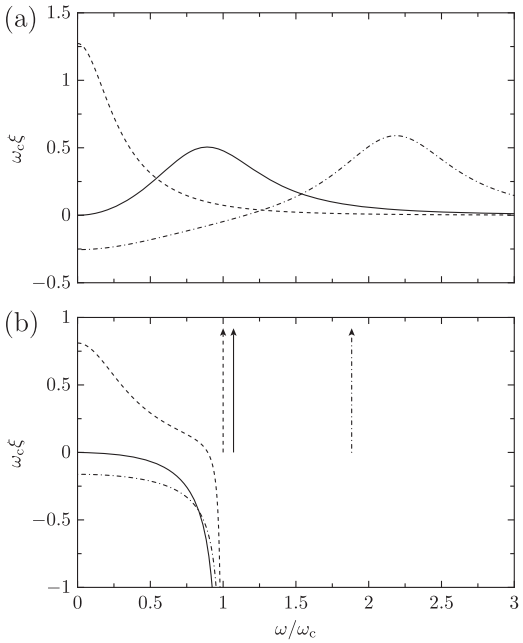

Figure 3. The change of the oscillator density of states is shown for an Ohmic environment (a) with an algebraic cutoff with $p = 1$ and (b) with a sharp cutoff. The dashed, solid, and dashed–dotted curves correspond to $\gamma/\gamma^\star = 0.2$, 1, and 5, respectively. In panel (b), the arrows indicate the positions of the delta function in (62).

already at the smaller value $\gamma \approx 0.322\ldots$ Correspondingly, the curve for $\gamma = 0.2$ has a negative curvature at $\omega = 0$ while the curves for $\gamma = 1$ and 5 have positive curvature.

For later reference, we note that at low frequencies the change of the oscillator density of states for super-Ohmic damping with $s = 3$ and an algebraic cutoff with $p = 2$ follows from (54) as

$$\xi_{\rm ac}(\omega) = -\frac{2\gamma}{\pi(2+\gamma)} + \frac{48\gamma + 12\gamma^2 + 2\gamma^3}{\pi(2+\gamma)^3}\,\omega^2. \tag{61}$$

3.3. Model II

For the spectral density of the coupling with a sharp cutoff (24), the CODS $\xi(\omega)$ is a continuous function of ω in the range $0 \leqslant \omega < 1$. For $\omega > 1$, the real part of the spectral damping function $\tilde{\gamma}(\omega)$ vanishes. Hence the density $\xi(\omega)$ is zero in this frequency range, except at a particular frequency $\omega = \Omega$, where the density $\xi(\omega)$ is singular. We thus have

$$\xi(\omega) = \xi_1(\omega) + \delta(\omega - \Omega), \tag{62}$$

where $\xi_1(\omega)$ is the smooth change of the oscillator density of states in the frequency range $0 \leqslant \omega < 1$,

$$\xi_1(\omega) = \frac{1}{\pi}\frac{g'(\omega)}{1 + g(\omega)^2}\Theta(1-\omega). \tag{63}$$

Employing the expression (26) for $\hat{\gamma}(z)$, the function $g(\omega)$ for $0 \leqslant \omega < 1$ reads

$$g(\omega) = -\cot\left(\frac{\pi s}{2}\right) + \frac{1}{\gamma}\omega^{2-s} - \frac{2}{\pi(2-s)}\omega^{2-s}\,{}_2F_1\left(1,\,1-\tfrac{s}{2};\,2-\tfrac{s}{2};\,\omega^2\right). \tag{64}$$

With this particular form, the sum rule for the partial density $\xi_1(\omega)$ is found as

$$\Sigma_1(s) = -\frac{s}{2}\,\Theta(2-s) - \Theta(s-2). \tag{65}$$

We see from the general expression (41) with (40) that the frequency $\Omega > 1$, at which the function $\xi(\omega)$ is singular, is a zero of the function

$$N(\omega, s) \equiv \omega - \operatorname{Im}\tilde{\gamma}(\omega) = \omega - \frac{2\gamma}{\pi s}\,\frac{{}_2F_1\left(1,\,\frac{s}{2};\,1+\frac{s}{2};\,\frac{1}{\omega^2}\right)}{\omega}. \tag{66}$$

In the particular cases $s = 1$ and $s = 3$ there holds

$$N(\omega, 1) = \omega - \frac{2\gamma}{\pi}\operatorname{arcoth}(\omega),$$
$$N(\omega, 3) = \omega\left(1 + \frac{2\gamma}{\pi}\right) - \frac{2\gamma}{\pi}\omega^2\operatorname{arcoth}(\omega). \tag{67}$$

The singular term in (62) contributes unity to the integrated change of the oscillator density of states. Hence the sum rule for the total change of the density of bath oscillators

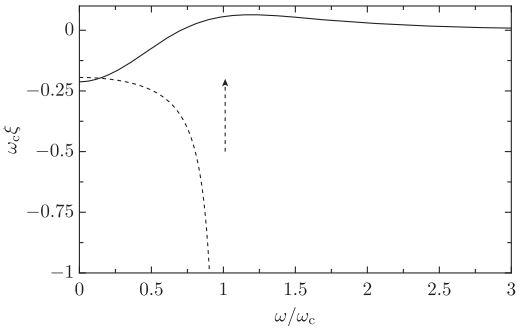

Figure 4. The change of the oscillator density of states is shown for a super-Ohmic environment with $s = 3$ and $\gamma = \omega_c$ with an algebraic cutoff with $p = 2$ (solid curve) and with a sharp cutoff (dashed curve). The arrow indicates the position of the delta function in (62).

(62) is

$$\Sigma(s) = \Sigma_1(s) + 1 = \left(1 - \frac{s}{2}\right)\Theta(2-s), \tag{68}$$

which is in full agreement with the corresponding expression (56) of model I.

The explicit expression for the low-frequency expansion of the change of the oscillator density (45) for model II follows from (46) and (47) together with (44), (30) and (31). As for model I, the leading term $n = 0$ in the expression (45) is positive for $\gamma < \gamma^\star$ and negative for $\gamma > \gamma^\star$. The coefficient c does not depend on γ at all and is found to read

$$c_{\rm sc}(s) = c_{\rm sc}^\star(s) = -\frac{2}{\pi^2}\sin^2\left(\tfrac{\pi s}{2}\right). \tag{69}$$

While the first term in (45) for both models depends only on the form of the cutoff through the critical damping strength $\gamma^\star$, the coefficient $c^\star$ in the expression (48) behaves qualitatively different for the two models. The coefficient $c_{\rm ac}^\star$ of model I given in (58) is generally positive, whereas the coefficient $c_{\rm sc}^\star$ of model II is generally negative.

The CODS $\xi(\omega)$ for model II is shown in figure 3(b) for Ohmic damping, $s = 1$. In this case, the critical damping strength is $\gamma_{\rm sc}^\star = \pi/2$, and the expression (50) takes the form

$$\xi(\omega) = \frac{1}{\pi}\left(\frac{1}{\gamma} - \frac{1}{\gamma_{\rm sc}^\star}\right) - \frac{1}{\pi}\left[\frac{1}{\gamma_{\rm sc}^*} + \left(\frac{1}{\gamma} - \frac{1}{\gamma_{\rm sc}^\star}\right)^3\right]\omega^2. \tag{70}$$

In contrast to the expression (60) for the algebraic cutoff, the curvature at small frequencies is negative for arbitrary damping strength γ. The different characteristics of $\xi(\omega)$ at low frequencies displayed in figures 3(a) and (b) are reproduced by the expressions (60) and (70).

The difference in curvature of the function $\xi(\omega)$ at zero frequency in models I and II also prevails for super-Ohmic damping with $s = 3$, as is clearly visible in figure 4. The qualitative difference between model I (solid curve) and model II (dashed curve) in figure 4 can be understood from the leading terms of the low-frequency series of $\xi(\omega)$ for $s = 3$

given in (54). The low-frequency expansion of the change of the oscillator density of states for model I is given in (61). For model II, we obtain from (54) together with (30), (31) and (44)

$$\xi_{\mathrm{sc}}(\omega) = -\frac{\gamma}{\pi + 2\gamma} - \gamma^2 \frac{6\pi + \left(12 - \pi^2\right)\gamma}{(\pi + 2\gamma)^3}\omega^2. \tag{71}$$

Importantly, the different sign of the curvature in models I and II displayed in (61) and (71), respectively, holds for general damping strength γ.

4. Reduced partition function and specific heat

Within the present paper, we determine thermodynamic quantities of open systems on the basis of the reduced partition function (1). For a free particle, the partition function is only well defined if the particle is confined to a finite region.

In the absence of an environmental coupling, we can evaluate the partition function of a particle confined to a one-dimensional infinite square well of width L and inner potential $V_0 = 0$. The corresponding eigenenergies are given by $E_n = E_{\mathrm{g}} n^2$ with $E_{\mathrm{g}} = \pi^2/2ML^2$ so that the partition function reads

$$\mathcal{Z}_0 = \sum_{n=1}^{\infty} \exp\left(-\frac{E_{\mathrm{g}}}{T} n^2\right) = \frac{1}{2}\left[\vartheta_3\left(0, \mathrm{e}^{-E_{\mathrm{g}}/T}\right) - 1\right]. \tag{72}$$

Here, $\vartheta_3(0, x)$ is a Jacobi theta function [15]. In the temperature regime

$$T > E_0 = cE_{\mathrm{g}}, \tag{73}$$

where c is a positive number sufficiently large so that for T above E_0 the discreteness of the energy eigenstates may be disregarded, the sum in the partition function can be turned into an integral. We thus arrive at the classical partition function of the undamped free particle

$$\mathcal{Z}_{0,\mathrm{cl}} = \sqrt{\frac{T}{E_{\mathrm{g}}}} \int_0^{\infty} \mathrm{d}x \, \exp\left(-x^2\right) = \sqrt{\frac{\pi T}{4E_{\mathrm{g}}}}. \tag{74}$$

This result depends only on the combination TL^2 and therefore is valid even for very low temperatures provided the particle is constrained to a sufficiently large region. How the confinement to a finite region influences the thermodynamic properties at very low temperatures, can for example be seen by studying a damped particle in a weakly confining harmonic potential [20].

For a damped particle, the partition function is augmented by quantum fluctuations due to the bath coupling. The accessory part may be written as an infinite Matsubara product [12] which, under the condition (73), does not depend on the width L of the square well. The resulting reduced partition function reads

$$\mathcal{Z} = \sqrt{\frac{\pi T}{4E_{\mathrm{g}}}} \prod_{n=1}^{\infty} \frac{\nu_n}{\nu_n + \hat{\gamma}(\nu_n)}, \quad T > E_0, \tag{75}$$

in which $\nu_n = 2\pi T n$ is a bosonic Matsubara frequency. The subsequent thermodynamic analysis is based on the expression (75).

The specific heat follows from the reduced partition function by

$$C = \frac{\partial}{\partial T}\left(T^2 \frac{\partial \ln(\mathcal{Z})}{\partial T}\right). \tag{76}$$

Based on the Matsubara representation (75), one finds

$$C = \frac{1}{2} + \sum_{n=1}^{\infty} y(\nu_n) \tag{77}$$

with the function [19]

$$y(\nu) = \left(\frac{\hat{\gamma}(\nu) - \nu\hat{\gamma}'(\nu)}{\nu + \hat{\gamma}(\nu)}\right)^2 - \frac{\nu^2\hat{\gamma}''(\nu)}{\nu + \hat{\gamma}(\nu)}, \tag{78}$$

where the prime denotes again the derivative.

The Matsubara series (77) is advantageous for moderate-to-high temperatures. From it we can immediately infer that C tends to 1/2 as $T \to \infty$. Regrettably, it is badly converging at low temperatures. In the latter regime, it is pertinent to perform a Poisson resummation of the series (77) by virtue of the periodically continued δ-function:

$$\delta(\tau) := T \sum_{n=-\infty}^{\infty} \exp\left(\mathrm{i}\nu_n \tau\right) \tag{79}$$

into the form

$$C = \frac{1}{2} - \frac{y(0)}{2} + \frac{1}{2\pi T}\int_0^{\infty} \mathrm{d}\nu \, y(\nu) + \frac{1}{\pi T}\sum_{n=1}^{\infty}\int_0^{\infty} \mathrm{d}\nu \, \cos\left(n\frac{\nu}{T}\right) y(\nu). \tag{80}$$

Since the antiderivative

$$Y(\nu) = \frac{\nu\left[\hat{\gamma}(\nu) - \nu\hat{\gamma}'(\nu)\right]}{\nu + \hat{\gamma}(\nu)}. \tag{81}$$

of the function $y(\nu)$ vanishes at the boundaries $\nu = 0$ and $\nu = \infty$, the first integral in (80) is strictly zero. In addition, the trigonometric function in the second integral of (80) is increasingly oscillating as $T \to 0$. Hence the second integral approaches zero in this limit. Thus the specific heat (80) can be expressed in the form

$$C = C_0 + \frac{1}{\pi T}\sum_{n=1}^{\infty}\int_0^{\infty} \mathrm{d}\nu \, \cos\left(n\frac{\nu}{T}\right) y(\nu), \tag{82}$$

where

$$C_0 = \frac{1}{2} - \frac{y(0)}{2} \tag{83}$$

is the specific heat at zero temperature. We find from (78) both with the form (19) and the form (29) for the spectral

damping function the limiting expression

$$y(0) = (2 - s)\Theta(2 - s). \tag{84}$$

The second term in (82) describes the temperature dependence of the specific heat and can serve to obtain low-temperature expansions.

A more physical interpretation of the specific heat for a damped system can be given in terms of the change $\xi(\omega)$ of the oscillator density of states caused by the coupling of the system to the heat bath [11], which has been discussed in section 3. Under the condition (16) the Matsubara sum (77) can be rewritten as the frequency integral

$$\begin{aligned} C &= \frac{1}{2} + \int_0^\infty \mathrm{d}\omega\, \xi(\omega)\big[C_{\mathrm{ho}}(\omega) - 1\big], \\ &= C_0 + \int_0^\infty \mathrm{d}\omega\, \xi(\omega)\, C_{\mathrm{ho}}(\omega). \end{aligned} \tag{85}$$

Here,

$$C_{\mathrm{ho}}(\omega) = \left(\frac{\omega}{2T\,\sinh(\omega/2T)}\right)^2 \tag{86}$$

is the specific heat of a single harmonic oscillator with frequency ω. Since in the high-temperature limit, C_{ho} tends to one, the first term on the right-hand side of the first line of (85) represents the classical value of the specific heat. On the other hand, in the low-temperature limit, C_{ho} tends to zero, thus confirming that C_0 is the specific heat at zero temperature. By comparing the first and the second line, we find that the specific heat in the zero-temperature limit

$$C_0 = \frac{1}{2} - \Sigma \tag{87}$$

is related to its classical value by the integrated CODS Σ introduced in (42).

With the explicit form (56) for the sum rule Σ, the expression (87) in fact coincides with the former result (83) with (84). In any event, the resulting expression for the specific heat at zero temperature is

$$C_0 = \begin{cases} \dfrac{s-1}{2} & \text{for } s \leqslant 2, \\ \dfrac{1}{2} & \text{for } s > 2. \end{cases} \tag{88}$$

In the regime $s \leqslant 2$, C_0 increases linearly with the exponent s from a value of $-1/2$ in the extreme sub-Ohmic regime to the classical value of $1/2$ which is reached for $s = 2$.

The expressions for the specific heat given in (85) differ from the expression which can be derived from the formula for the free energy given by Ford *et al* [21, 22] for the damped harmonic oscillator. The reason lies in the nonvanishing specific heat of the free damped particle at zero temperature.

Figure 5 gives an overview of typical variations of the specific heat of a damped free particle as a function of temperature. In order to emphasize that the represented data are only valid as long as the condition (73) is satisfied, i.e. provided that TL^2 is sufficiently large, we denote the leftmost value on the temperature axis by 0^+. The three curves represent a sub-Ohmic case ($s = 0.3$), the Ohmic case ($s = 1$) and a super-Ohmic case ($s = 3$) from the lower to the upper curve. In all cases, a sharp cutoff (model II) has been employed.

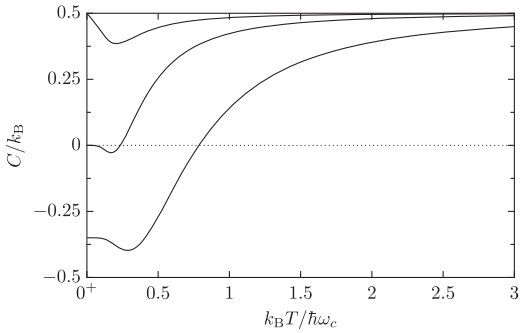

Figure 5. The specific heat (77) of a free damped particle is displayed as a function of temperature for spectral densities of the coupling (24) with a sharp cutoff. The label 0^+ on the temperature axis indicates that the curves are only valid for $k_{\mathrm{B}}T > E_0$. The exponent s increases from the lower to the upper curve as $s = 0.3$, 1, and 3. For the two smaller values of s, the critical damping strength $\gamma = \gamma_{\mathrm{sc}}^\star$ is chosen while for $s = 3$ the damping strength is set to $\gamma = 1$.

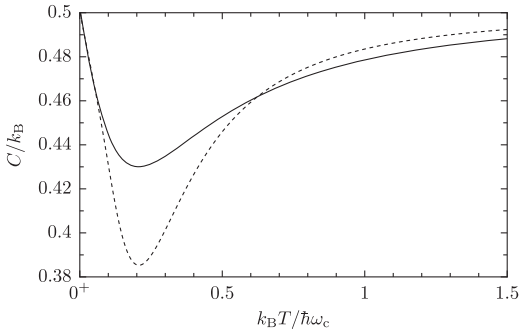

Figure 6. The specific heat is shown for super-Ohmic damping $s = 3$ with an algebraic cutoff with $p = 2$ (solid curve) and a sharp cutoff (dashed curve). The damping strength for both curves is $\gamma = 1$. The dashed curve is a magnified form of the topmost curve in figure 5. We see that the dip in the specific heat is notably larger for model II compared with model I.

As our previous analysis has shown, all three curves lead from a zero-temperature value of the specific heat given by (88) to the classical value $k_{\mathrm{B}}/2$. The Ohmic case is a particular case because it leads to a vanishing specific heat in the zero-temperature limit independently of any confinement condition for the particle. In the sub-Ohmic case, the specific heat at low temperatures tends towards a negative value.

In contrast, for super-Ohmic damping with $s > 2$, which includes the case $s = 3$ represented in figure 5, at low temperatures the classical value of the specific heat is approached again. This phenomenon of reentrant classicality is due to the small density of bath oscillators at low frequencies [19]. In figure 6 the reentrant classicality for the super-Ohmic case $s = 3$ is shown both for model I and model II. The dip in the specific heat due to quantum effects is considerably larger in the dashed curve belonging to model II compared with the solid curve pertaining to model I. The discriminative characteristics in figure 6 is due to the drastically different behaviors of the CODS $\xi(\omega)$ of these models shown in

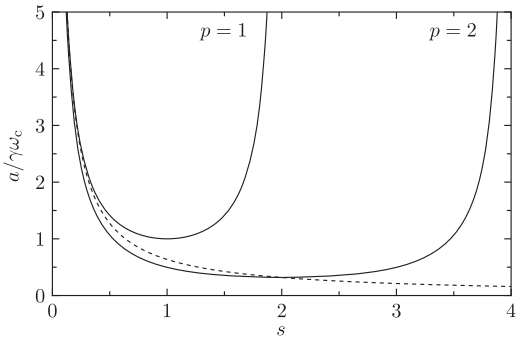

Figure 7. The amplitude functions $a_{ac}(s, p)$ for algebraic cutoffs characterized by exponents $p = 1$ and $p = 2$ (solid curves) and the amplitude function $a_{sc}(s)$ for sharp cutoff (dashed curve) appearing in the high-temperature formula (89) are shown as a function of the exponent s.

figure 4. It should be remarked, that the dip for both models gets deeper, as the parameter γ is increased, while the characteristics of reentrant classicality is preserved.

As far as the two lower curves in figure 5 belonging to the range $0 < s < 2$ are concerned, their dips get progressively deeper, as the damping strength γ is increased beyond $\gamma^\star$ [19]. This feature is due to the negative sign of the leading term in the expansion (45) in the regime $\gamma > \gamma^\star$.

The overall structure discussed so far only depends on the exponent s of the spectral density of the coupling and is thus independent of the cutoff. The cutoff becomes relevant though at finite temperatures. Accessible to a analytical analysis are the leading quantum corrections at high temperatures which we will discuss in section 5 and the low-temperature expansion which will be the subject of section 6. The low-temperature behavior is particularly interesting because for sufficiently strong coupling of the free particle to its environment, the specific heat at finite temperatures can fall even below its zero-temperature value.

5. Quantum corrections at high temperatures

The specific heat at temperatures $T \gg \gamma, \omega_c$ is determined by the behavior of the Laplace transform $\hat{\gamma}(z)$ of the damping kernel in the regime $|z| \gg 1$, which is given in equation (17). In the high-temperature regime, the Matsubara sum (77) is dominated by the second term in (78). As the damping kernel decays like $1/z$ for all exponents s in the range (16), the leading quantum correction at high temperatures then goes like the square of the inverse temperature.

$$C = \frac{1}{2} - \frac{a}{12}\frac{1}{T^2}. \tag{89}$$

The coefficient a is given in (18) for model I and in (28) for model II.

The universal $1/T^2$ tail is proportional to the damping strength γ and, after reinserting the constants previously set to one, the cutoff frequency ω_c. The amplitude functions $a_{ac}(s, p)/\gamma$ for model I and $a_{sc}(s)/\gamma$ for model II are plotted in figure 7. The U-shaped form for model I (displayed for $p = 1$ and $p = 2$) possesses a minimum at $s = p$ and divergencies at the edges $s = 0$ and $s = 2p$. For a given algebraic cutoff function characterized by p, quantum effects can depend significantly on the value of the exponent s. They are weakest for $s = p$.

When, on the other hand, s is kept fixed, the function $a_{ac}(s, p)$ decreases with increasing parameter p. Thus, sharpening the cutoff function in the spectral density of the coupling (6) in model I reduces the quantum effects while the temperature is kept fixed at a large value.

For the sharpest possible cutoff function, i.e. our model II, the amplitude a_{sc} decreases monotonically as $1/s$ with increasing exponent s. Although, the sharp cutoff does in general not lead to the smallest high-temperature quantum corrections, it nevertheless fits the general picture that sharper cutoffs in the spectral density of the coupling tend to lead to weaker quantum corrections.

6. Low-temperature behavior

We finally study the low temperature regime where T provides the smallest frequency scale, i.e. $T \ll \gamma, \omega_c$. As mentioned before, for a particle confined to a finite spatial region, our results are constrained by the condition (73) and are thus not valid down to zero temperature. However, by choosing the confining region sufficiently large, the domain of validity can be extended down to any arbitrarily low non-zero temperature. The low-temperature expansions for the specific heat given in this section have to be understood in this sense.

The leading low-temperature correction to the specific heat is obtained from the leading low-frequency term in the change of the oscillator density of states $\xi(\omega)$ discussed in section 3.1. In the regime $0 < s < 2$, the leading contribution to the CODS $\xi(\omega)$ is found to be proportional to ω^{1-s}. From the expression for the specific heat in the second line of (85), we obtain the leading low-temperature behavior of the specific heat as

$$C = \frac{s-1}{2} + \frac{2-s}{\pi}\left(\frac{1}{\gamma} - \frac{1}{\gamma^\star}\right) \times \sin^2\left(\tfrac{\pi s}{2}\right)\Gamma(4-s)\zeta(3-s)T^{2-s}. \tag{90}$$

Here, ζ denotes the Riemann zeta function [15]. The expansion (90) depends mainly on the low-frequency dependence of the spectral density of the coupling. Its dependence on the form of the cutoff enters only via the critical damping strength $\gamma^\star$.

The leading low-temperature correction to the specific heat increases with decreasing damping strength γ. Consequently, a reduction of the environmental coupling leads to a more rapid approach to the classical regime as temperature is increased. This behavior is consistent with the fact that in the absence of any spatial confinement, the environmental coupling provides the mechanism to render a free particle quantum mechanical [1, 9, 19].

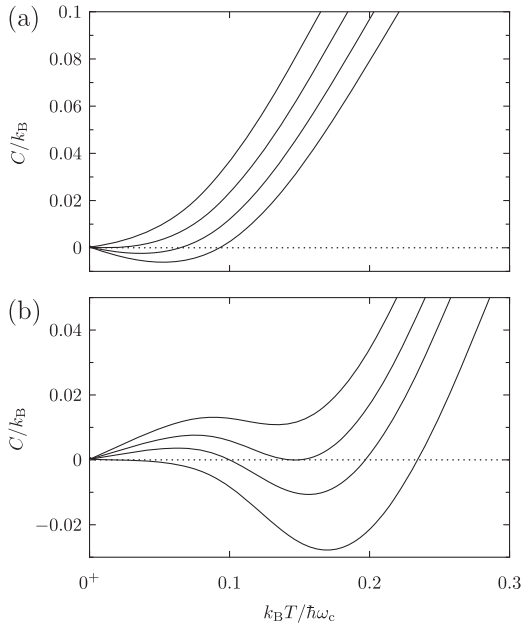

Figure 8. The specific heat at low temperatures where negative values can occur is shown for Ohmic damping with (a) an algebraic cutoff with $p = 1$ and (b) a sharp cutoff. In the upper panel, the damping strength $\gamma/\omega_c = 0.9$, 1, 1.1, and 1.2 increases from the upper to the lower curve. The second value represents the critical damping strength $\gamma = \gamma^\star_{ac}$. In the lower panel, the damping strength takes the values $\gamma/\omega_c = 1.2$, 1.3, 1.4, and $\pi/2$ from the upper to the lower curve. The last choice corresponds to $\gamma = \gamma^\star_{sc}$. We see that already for values $\gamma < \gamma^\star_{sc}$ the specific heat can become negative at finite temperatures.

With increasing damping strength, eventually the critical damping strength $\gamma^\star$ will be reached where the dressed mass $M(1 + \mu)$ vanishes. According to (45), the leading term of $\xi(\omega)$ then changes sign and the leading low-temperature correction results in a decrease of the specific heat with increasing temperature. In figure 8(a), we show the low-temperature behavior of the specific heat for Ohmic dissipation with an algebraic cutoff with $p = 1$. The damping strength in figure 8(a) increases from the upper to the lower curve, clearly demonstrating the change in the sign of the leading term in the CODS $\xi(\omega)$ at the critical damping strength represented by the second curve from the top.

Interestingly, the low-temperature behavior for a sharp cutoff shown in figure 8(b) is qualitatively different. While we see again how the leading term in (45) changes its sign when the critical damping strength is reached at the lowest curve, a negative specific heat can be obtained even for damping strengths below the critical damping strength. However, the specific heat falls below its zero-temperature value only above a certain finite temperature.

This difference in behavior of the specific heat for algebraic and sharp cutoff can be traced back to the coefficient c in the expansion (45). This coefficient dominates the low-temperature behavior of the specific heat at the critical damping strength $\gamma = \gamma^\star$, where the first term in (45) vanishes. The specific heat then reads

$$C = \frac{s-1}{2} + c^\star\, \Gamma(6-s)\zeta(5-s)T^{4-s}, \tag{91}$$

where the coefficient $c^\star$ is given in (58) for model I and in (69) for model II. Recalling the discussion at the end of section 3.3, the leading thermal contribution for critical damping $\gamma = \gamma^\star$ is generally positive for model I and generally negative for model II. For a sharp cutoff, the absolute value of the coefficient c can be large enough, even for undercritical damping $\gamma < \gamma^\star$, to force the specific heat below zero as can be seen in figure 8(b).

In the regime $s > 2$, we had seen from (88) that at zero temperature, the specific heat takes it classical value. Upon using the expression (51) for the change of the oscillator density of states $\xi(\omega)$, we find that the leading contribution to the specific heat at low temperatures is

$$C = \frac{1}{2} - (s-2)\frac{\gamma}{\pi(1+\mu)}\Gamma(s)\zeta(s-1)T^{s-2}. \tag{92}$$

Interestingly, details of the cutoff in the spectral density of the coupling $J(\omega)$ only enter via the mass renormalization μ. The leading thermal contribution in (92) is always negative, thereby ensuring that the specific heat never exceeds its classical value.

7. Conclusions

The thermodynamic properties of a damped quantum system depend on the spectral density of the coupling, in particular its low-frequency behavior and the high-frequency cutoff. Choosing a rather general spectral density of the form (10), we have seen for the specific heat of the free damped particle, that the exponent s characterizing the low-frequency properties of the environmental coupling is omnipresent. Nevertheless, also the existence of the high-frequency cutoff and its detailed form are of relevance.

First of all, the negative mass renormalization in the regime $0 < s < 2$ is a consequence of the mere existence of a high-frequency cutoff. In this sense, the possibility for the specific heat to fall below its zero-temperature value constitutes an effect of the cutoff. Typically, this requires that damping strength and cutoff frequency are of the same order which makes the appearance of cutoff effects likely. However, as we have seen in figure 2, there exist parameter ranges where even relatively weak damping can lead to a decrease of the specific heat at low temperatures.

A qualitative difference between the two types of cutoffs considered here, i.e. the algebraic cutoff (11) and the sharp cutoff (24), can be found in the change of the oscillator density of states when the system degree of freedom is coupled to the bath. At low frequencies, the curvature of the CODS is always negative for a sharp cutoff while it is positive for an algebraic cutoff in the regime where the specific heat becomes negative.

Quantitative differences appear in the details of the relevant quantities, e.g. the expressions for the mass renormalization or the critical damping strength. While the general form of the expressions for the two types of cutoff are similar, important differences are due to the fact that for a given algebraic cutoff, the allowed values of the low-frequency exponent s are limited by the conditions (12) or (16). As a consequence, the mass renormalization and the amplitude of the high-temperature quantum corrections for the algebraic cutoff are nonmonotonic and divergent at $s = 2p$. In contrast, the sharp cutoff is sufficiently strong to allow for arbitrary values of s. The corresponding mass renormalization and the quantum corrections of order $1/T^2$ vanish in the limit of large exponents s.

Finally, we have seen in the discussion of the leading low-temperature corrections that while the critical damping strength typically determines whether the specific heat can fall below its zero-temperature value, this is not always the case. For the sharp cutoff, the results shown in figure 8(b) demonstrate that a negative specific heat in the Ohmic case can appear even before the critical damping strength is reached.

Acknowledgments

The authors would like to thank Peter Hänggi and Peter Talkner for stimulating discussions. One of us (UW) has received financial support from the Deutsche Forschungsgemeinschaft through SFB/TRR 21. GLI is grateful to the Laboratoire Kastler Brossel in Paris for its hospitality during the preparation of the manuscript.

References

[1] Hänggi P, Ingold G-L and Talkner P 2008 *New J. Phys.* **10** 115008
[2] Florens S and Rosch A 2004 *Phys. Rev. Lett.* **92** 216601
[3] Ingold G-L, Lambrecht A and Reynaud S 2009 *Phys. Rev.* E **80** 041113
[4] Žitko R and Pruschke T 2009 *Phys. Rev.* B **79** 012507
[5] Campisi M, Talkner P and Hänggi P 2009 *J. Phys. A: Math. Theor.* **42** 392002
[6] Campisi M, Zueco D and Talkner P 2010 *Chem. Phys.* **375** 187
[7] Sulaiman A, Zen F P, Alatas H and Handoko L T 2010 *Phys. Rev.* E **81** 061907
[8] Merker L and Costi T 2012 *Phys. Rev.* B **86** 075150
[9] Hänggi P and Ingold G-L 2006 *Acta Phys. Pol.* B **37** 1537
[10] Ingold G-L, Hänggi P and Talkner P 2009 *Phys. Rev.* E **79** 061105
[11] Ingold G-L 2012 *Eur. Phys. J.* B **85** 30
[12] Weiss U 2012 *Quantum Dissipative Systems* 4th edn (Singapore: World Scientific)
[13] Hakim V and Ambegaokar V 1985 *Phys. Rev.* A **32** 423
[14] Grabert H, Schramm P and Ingold G-L 1988 *Phys. Rep.* **168** 115
[15] Olver F W J, Lozier D W, Boisvert R F and Clark C W (ed) 2010 *NIST Handbook of Mathematical Functions* (New York: Cambridge University Press)
[16] Schramm P and Grabert H 1987 *J. Stat. Phys.* **49** 767
[17] Bao J-D, Hänggi P and Zhuo Y-Z 2005 *Phys. Rev.* E **72** 061107
[18] Grabert H, Schramm P and Ingold G-L 1987 *Phys. Rev. Lett.* **58** 1285
[19] Spreng B, Ingold G-L and Weiss U 2013 *Europhys. Lett.* **103** 60007
[20] Adamietz R, Ingold G-L and Weiss U 2014 *Eur. Phys. J.* B **87** 90
[21] Ford G W, Lewis J T and O'Connell R F 1985 *Phys. Rev. Lett.* **55** 2273
[22] Ford G W, Lewis J T and O'Connell R F 1988 *Ann. Phys., NY* **185** 270